Decoupled length scales for diffusivity and viscosity in glass-forming liquids

H. L. Peng[1,*] and Th. Voigtmann[1,2]
[1]*Institut für Materialphysik im Weltraum, Deutsches Zentrum für Luft- und Raumfahrt (DLR), 51170 Köln, Germany*
[2]*Department of Physics, Heinrich-Heine-Universität Düsseldorf, Universitätsstraße 1, 40225 Düsseldorf, Germany*
(Received 29 July 2016; published 26 October 2016)

The growth of the characteristic length scales both for diffusion and viscosity is investigated by molecular dynamics utilizing the finite-size effect in a binary Lennard-Jones mixture. For those quantities relevant to the diffusion process (e.g., the hydrodynamic value and the spatial correlation function), a strong system-size dependence is found. In contrast, it is weak or absent for the shear relaxation process. Correlation lengths are estimated from the decay of the spatial correlation functions. We find the length scale for viscosity decouples from the one of diffusivity, featured by a saturated length even in high supercooling. This temperature-independent behavior of the length scale is reminiscent of the unapparent structure change upon supercooling, implying the manifestation of configuration entropy. Whereas for the diffusion process, it is manifested by relaxation dynamics and dynamic heterogeneity. The Stokes-Einstein relation is found to break down at the temperature where the decoupling of these lengths happens.

DOI: 10.1103/PhysRevE.94.042612

I. INTRODUCTION

If nucleation is avoided, upon cooling to the glass transition temperature the structural relaxation time of liquids increases by several orders of magnitude. A crucial question is how the spatial correlation length behaves in this sluggish process. One of the most famous theories to explain the glass transition is the mode coupling theory (MCT) [1]. In this theory, the origin of the dynamic slowdown is the structural frustration upon approaching density jamming points, when the atoms become trapped by their nearest neighbours. Thus, the only relevant length scale in MCT is the atomic cage size. Predictions of this theory have been validated by several experimental and numerical results [2,3]. Discrepancies become significant near the crossover temperature T_c, where the dynamics of system should be completely frozen according to simple MCT, in contradiction to experimental results and computer simulation. Below T_c, the dynamics of the system, despite being sluggish, can still relax through cooperative motion of small groups of atoms, e.g., jump or stringlike movement [4]. In this region, the fluctuation of dynamics is strongly spatiotemporal inhomogeneous, i.e., it shows the so-called dynamic heterogeneity (DH) [5–9]. The length scale for this heterogeneous fluctuations increases drastically near T_c and exceeds the typical length scale of an atomic cage [10–14].

The emergence of atomic collective movements in space and time leads to many abnormal phenomena in transport processes. For instance, upon supercooling, the diffusion coefficients and the shear viscosity exhibit a clear transition from simple exponential to stretched exponential decay, i.e., an Arrhenius to non-Arrhenius transition at a temperature above T_c [15–17]. Also in this transition, the Stokes-Einstein relation (SER), which formulates a simple relation between single-particle diffusion and cooperative relaxation of the surrounding solvent, breaks down [17,18]. In view of thermally activated processes, the non-Arrhenius behavior, i.e., D or $1/\eta \sim \exp[E_A(T)/k_BT]$, indicates a change of the activation volume due to the temperature dependence of the activation energy. A plausible speculation is that this volume would be consistent with that of dynamic heterogeneity, and then all these abnormal phenomena can be rationalized by the DH [17,19].

One way to realize this speculation is by empirically scaling the diffusivity and/or structure relaxation time with the correlation length. A commonly used formula for this scaling includes a conventional power law, $A \sim \xi^w$, and a thermoactivation behavior, $\log(A) \sim \xi^v$ (A could be relaxation the time, viscosity, or diffusivity). The correlation length, ξ, is usually calculated as the four-point correlation length that evaluates the dynamic heterogeneity, or the point-to-set correlation length measured through the pinning protocol [5,20]. The exponents for this empirical scaling differ from system to system and even differ for relaxation time and diffusion in the same system [13,21,22]. Another more physically meaningful approach is from generalized hydrodynamics. One quantity is the wave-vector-dependent viscosity or viscosity in a generalized Stokes-Einstein relation [23,24]. The length scale determined from this has been reported to coincide with that of the dynamic heterogeneity [25,26]. Another quantity is the wave-vector-dependent diffusivity. The corresponding length scale accounts for the crossover from Fickian to non-Fickian diffusion [27,28]. Recently, researchers have attempted to scale diffusivity and shear viscosity (or structural relaxation time) by a single correlation length, coinciding with the one of the DH [26]. However, it is still unclear why diffusivity and viscosity should couple with the same correlation length, since a slow subsystem where the SER holds would exist in undercooling [29,30].

At high temperatures, there is no controversy that the length scales for all these processes, i.e., dynamic heterogeneity, diffusivity, and viscosity, are all correlated and the same as the atomic diameter—the only relevant length scale in dilute liquids. Upon supercooling, the situation becomes more complicated because of the constraint of the dynamic fluctuations

*Corresponding author: hailong.peng@dlr.de

by the potential energy landscape. The complex shape of the potential energy landscape makes the ergodicity of the system temperature dependent and eventually relaxation processes (e.g., α and β relaxations) decouple from each other [31,32]. As a consequence, multiple length and time scales are found in the glass-forming liquids [33,34]. A noticeable example of the multiple length scales is the decorrelation of static and dynamic correlation length upon supercooling. The static correlation length can be calculated in three different ways: local-order correlation (e.g., bond orientation order), point-to-set correlation (via random pinning or wall frozen protocol), and structural frustration methods. Despite some consistent results found for the same correlation lengths for dynamic heterogeneity and bond orientational order [35,36], a discrepancy between the static and dynamic lengths has been reported for all these methods (see Refs. [21,37], [20,22,38], and [39,40] for the three methods, respectively). A common finding is that, with decreasing temperature (or density increasing), the dynamic length increases significantly faster than the static one.

Other than the relation of static and dynamic lengths, the length scales for diffusivity and viscosity have not been studied intensively, despite their importance for the understanding of the decoupling of the different relaxation processes. Via computer simulation, we will address this problem mainly by utilizing the finite-size effect.

Unlike the pinning or structural frustration method, the finite-size effect can detect underlying correlation lengths without perturbing the equilibrium fluctuations in real space. This method has been extensively used for the scaling of critical length when a system approaches a first-order or glass transition point [19,41,42]. The key point of it is that the size of the simulated box can be considered as an additional physical length, which directly interplays with the correlation length of the underlying physical processes. This effect is essentially important concerning collective movement; e.g., ignoring this effect would lead to an incorrect measurement of the length scale of the conventionally used four-point correlation function [43]. By utilizing this method, recent investigations have shown different system-size dependencies of structural relaxation time and dynamic susceptibility [44]. The correlation length extracted by the configuration entropy is found to be much shorter than the one of the dynamic heterogeneity.

In the following, we present a molecular dynamics simulation study for the length scales underlying diffusivity and viscosity in a binary Lennard-Jones mixture. The system-size dependency of diffusion and shear viscosity is interpreted in terms of their hydrodynamic values and the corresponding spatial correlation functions. Quantities related to the diffusion process show a much stronger system-size dependency than the shear relaxation process. Correlation lengths are also estimated by spatial correlation functions. We find that the length scale for viscosity decouples from the one of diffusion, distinguished by a saturated length scale in high supercooling. Consistently, the fluctuation of shear-stress field is found to limit about 8–10 atomic diameters, not growing up on further undercooling. The length scale required for the viscosity is attributed to the static configuration of liquids, while is the dynamic collectivity for the diffusion coefficient.

II. SIMULATION DETAILS

The molecular dynamics simulation is conducted using a Lennard-Jones potential with Kob-Anderson parameters [3]:

$$U_{\alpha\beta}(r) = 4\epsilon_{\alpha\beta}\left[\left(\frac{\sigma_{\alpha\beta}}{r}\right)^{12} - \left(\frac{\sigma_{\alpha\beta}}{r}\right)^{6} + A_{\alpha\beta}r + B_{\alpha\beta}\right],$$

where $\alpha,\beta \subseteq \{A,B\}$, $\sigma_{AA} = 1.0$, $\epsilon_{AA} = 1.0$, $\sigma_{AB} = 0.8$, $\epsilon_{AB} = 1.5$, $\sigma_{BB} = 0.88$, and $\epsilon_{BB} = 0.5$. Following common practice, the potential is truncated at $r = 2.5\sigma_{\alpha\beta}$. The parameters $A_{\alpha\beta}$ and $B_{\alpha\beta}$ ensure that the potential and its first derivative go smoothly to zero at the cutoff. The composition $A_{80}B_{20}$ is investigated due to its strong resistance against crystallization. All simulations are performed via the software package LAMMPS [45]. The equations of motion are integrated with a standard velocity-Verlet algorithm with a time step of 0.0015 at high temperatures ($T \geqslant 1$) and 0.003 otherwise. The samples are first constructed at high temperature ($T = 5$), then cooled down to the target temperature with the average pressure ($= 5.0$) fixed. At the target temperature, the samples are first equilibrated at NPT ensemble (i.e., constant particle number N, pressure P = 5.0, and constant temperature T) used to find the corresponding volume. Then we switch to an NVE ensemble (micro-canonical ensemble), when the data are collected after an additional relaxation. By this procedure, a clear cage effect is found in the system when $T \leqslant 0.8$ (featured as an observable second-step relaxation emerges in the self-intermediate scattering function at the wave-vector value of the first maximum in the static scattering function). The mode-coupling crossover temperature is found approximately at $T = 0.46$ (obtained by fitting of the temperature-dependent self-diffusion coefficient). A series of different particle numbers is used for the finite-size effect investigation, $N = 200$, 400, 800, 1600, 3000, 6000, 12 000, 24 000, 50 000, 100 000. To improve statistics, averages over several samples for each system size were taken (up to 50 samples averaged for small systems, down to 2 samples for the largest system).

A generalized form for the definition of a spatial correlation (or four-point correlation) function is

$$C_A(r,t) = \frac{\langle (A_i(t) - \bar{A})[A_j(t) - \bar{A}]\delta[r - |\vec{r}_i(0) - \vec{r}_j(0)|]\rangle}{\langle [A_i(t) - \bar{A}]^2\rangle \langle \delta[r - |\vec{r}_i(0) - \vec{r}_j(0)|]\rangle}, \tag{1}$$

where $A_i(t)$ is a local quantity of atomic attribute, i or j is the atomic index, and $\bar{A} = \langle A_i(t)\rangle$. For the displacement field correlation function $C_{\rm disp}$, $A_i(t) = |\vec{r}_i(t) - \vec{r}_i(0)|^2$. For the atomic-level shear stress correlation function $C_{\rm str}$, $A_i(t) = \sigma_i^{xy}(t) - \sigma_i^{xy}(0)$, where $\sigma_i^{xy} = m v_i^x v_i^y + \sum_j r_{ij}^x F_{ij}^y$, and F_{ij} is the force on atom i exerted by atom j.

III. RESULTS

A. Finite-size effect for transport coefficients

The diffusion coefficients are calculated through the Einstein relation $D_\alpha = \lim_{t\to\infty}\langle|\mathbf{r}_i^\alpha(t) - \mathbf{r}_i^\alpha(0)|^2\rangle/6t$, where α designates the atomic species. In normal liquids, the diffusion coefficients calculated by computer simulation are strongly affected by long-range interactions arising from

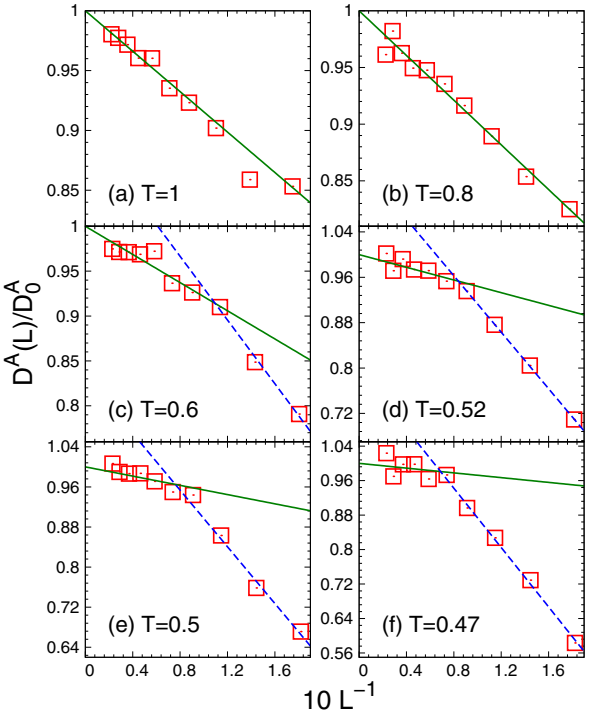

FIG. 1. System-size-dependent diffusion coefficient for particle A. The data are normalized by the factor D_0^A, which is the diffusivity for infinite system size, obtained via the fitting of formula 2 (solid green lines). Numbers of particles used for the points from right to left are $N = 200, 400, 800, 1600, 3000, 6000, 12\,000, 24\,000, 50\,000, 100\,000$.

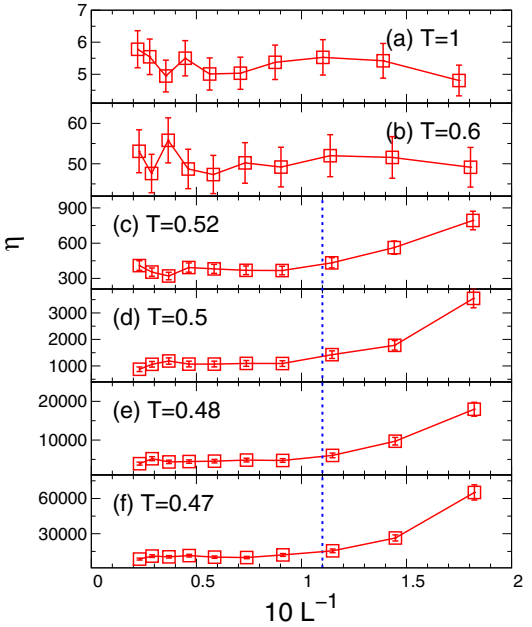

FIG. 2. System-size-dependent shear viscosity. The vertical dashed line is an estimation of the constant critical box length ($=9\,\sigma$) above which the finite-size effect disappears for all low-temperature liquids.

hydrodynamics [46]. The system-size-dependence of the self-diffusion coefficients due to hydrodynamic fluctuation has been described theoretically as [47,48]

$$D_L = D_0 - \frac{k_B T \xi}{6\pi \eta L}, \tag{2}$$

where $\xi = 2.837$ is a constant, L is the cubic box length, and η is the viscosity of the system. Notice that η is L independent in normal liquids (see Ref. [48]) or saturated for large-box-size systems in supercooled liquids (see viscosity data below) in this fragile liquid.

Utilizing this formula, we fit the system-size-dependent diffusion coefficients of particle A via the sole free parameter D_0 (the diffusivity for infinite system size). Results are shown in Fig. 1. In normal liquids ($T \geqslant 0.8$), the theoretical formula [Eq. (2)] describes the diffusion data well, from the smallest box size to the largest one (see green lines in Fig. 1). This changes at low temperatures ($T \leqslant 0.6$). The hydrodynamic description only fits to large systems. At low temperatures, it is known that the diffusion process cannot be considered as a single particle's movement, but some correlated motion for a group of atoms in the form of jump or stringlike movement [4,49]. If the simulation box size is comparable or smaller than the length of this collective movement, the diffusion process can be affected by strong self-interaction through the period boundary condition. A hydrodynamic description fails then, and the scaling behavior is governed by the constrained situation where the correlation length competes with the box length. This crossover gives clue to the upper limit of such a correlation length. As shown in Fig. 1, the crossover points, extracted from the intersection of hydrodynamic description (green lines) and the constrained situation (blue dashed lines), shift to larger and larger box sizes as the temperature decreases. This indicates a growing length scale required for the diffusion process, which would be due to the increase of number of atoms participating in stringlike movement.

The shear viscosity can be calculated in the equilibrium state through the Green-Kubo relation $\eta = V/(k_B T)\int_0^\infty \langle P_{xy}(t) P_{xy}(0)\rangle dt$, where V is the volume of the simulation box and P_{xy} is the off-diagonal pressure of the system. Results for the shear viscosity are shown in Fig. 2. At high temperatures ($T \geqslant 0.6$), no significant finite-size effect emerges within the error bars. At low temperatures, smaller systems exhibit a higher viscosity than the larger systems. In small systems, more degrees of freedom or relaxation channels are cut off by the finite box size. This leads to slower dynamics similar to the diffusion case shown in Fig. 1. A striking result is that the critical box size for the viscosity to reach the bulk value does not increase significantly in highly supercooled liquids, indicating a saturated length scale for viscosity upon supercooling. This saturation behavior, however, is in contrast to the length scale for diffusivity and dynamic heterogeneity. We stress the importance of this problem, as it indicates a nondiverging length scale when approaching the glass transition temperature. Due to the error bars of the viscosity calculation at low temperatures (up to 8%), the critical system box size where the size effect disappears is not exact (as shown in Fig. 2). We keep cautious on this point at this moment and will discuss it further down.

B. Spatial correlation functions

In order to get more detailed information about the correlation behavior in the diffusion and viscous processes, we turn to the measurement of spatial correlation functions. For the diffusion coefficient, the relevant quantity is the displacement field. The calculated spatial correlation function for atomic displacement is shown in Fig. 3. Here, we focus on the time scale τ_α, which is defined as the time when the dynamic susceptibility $\chi_4(t)$ reaches its maximum. Dynamic susceptibility is defined as $\chi_4(t) = 1/N[\langle W^2(t)\rangle - \langle W(t)\rangle^2]$, where $W(t) = \sum_i \Theta[a - |\vec{r}_i(t) - \vec{r}_i(0)|]$, $\Theta(x)$ is the Heaviside step function, and a is a constant (chosen as 0.3 here). By default, this time scale is also used in the following for the atomic level shear-stress field.

At high temperatures ($T > 0.6$), the correlation of the displacement field is nonzero only for short-range distance, with the strong oscillation attributed to density fluctuation. With decreasing temperature, this correlation survives for longer distances, indicating that more atoms move in a cooperative way. The spatial decay of the displacement correlation can be described by an exponential function, with the exponent giving the characteristic correlation length. This has been previously reported by measuring the collective movement of atoms [8,50–52]. Mathematically, if a correlation function decays exponentially as $\exp(-r/\xi)$, its Fourier transformation will be in the form of Lorentzian formula $\sim\xi/(1+q^2\xi^2)$. Thus, this spatial correlation function actually measures the same correlation behavior as the dynamic heterogeneity does [10–14]. As illustrated by the dash-dotted lines in Fig. 3, the characteristic length extracted from fitting shows an increase with decreasing temperature, or in other words, a tendency to diverge upon supercooling. We notice that if we define another correlation length as the distance where the correlation function decays to some finite value δ (e.g., $\delta = 10^{-4}$, for the largest system investigated), we will get a length scale approximately coinciding with the crossover critical box length in Fig. 1. Thus, the results for finite-size scaling and correlation function are consistent. This indicates the dynamic heterogeneity accounts for the breakdown of the hydrodynamic description [i.e., Eq. (2)], as the collectivity between atoms cannot be neglected at this time.

A pronounced negative correlation region can be found at low temperatures (when the sign of $C_{\rm disp}$ changes from positive to negative, the plot exhibits a dip as shown in the lower panels of Fig. 3). This anticorrelation is attributed to the well-known backflow, or vortex pattern, generated by the hydrodynamic fluctuation [53] and has been verified by the perpendicular part of this correlation function in a Brownian system [54]. An interesting phenomenon is that the size of the hydrodynamic vortex, i.e., the minimum length of anticorrelation, strongly depends on the box size in the simulation. For larger system sizes, the distance where the backflow happens is longer (or equivalently later). Thus, exponential fitting of the correlation functions in small systems will lead to smaller correlation lengths. This kind of underestimation has also been reported for length-scale calculations in Fourier space [14]. As an approximation, here we use the largest system, i.e., $N = 100\,000$, to measure the correlation length (result is shown in Fig. 6). The actual correlation length in an infinite system would be larger than the value we obtained. But the tendency to increase with undercooling will not change.

We now turn to the spatial correlation function for the atomic level shear stress, which is relevant to shear viscosity (see Sec. II for its definition). Due to propagation, the shear-stress correlation function oscillates around the abscissa (see Fig. 5). Again, we use the absolute value to make the semilog plot, shown in Fig. 4. Strikingly, the decay of the stress correlation is insensitive to the temperature (see Fig. 4). A characteristic length 1.2 σ can be considered as the upper limit of the correlation length for all investigated temperatures. This value is clearly lower than that of the displacement field. For the viscosity calculation, as the main contribution of it comes from virial part at low temperature, it could be the manifestation of the static structure and then possibly shares the same underlying correlation length. This result is consistent with the temperature-independent static length found in the structural frustration scenario [39,40].

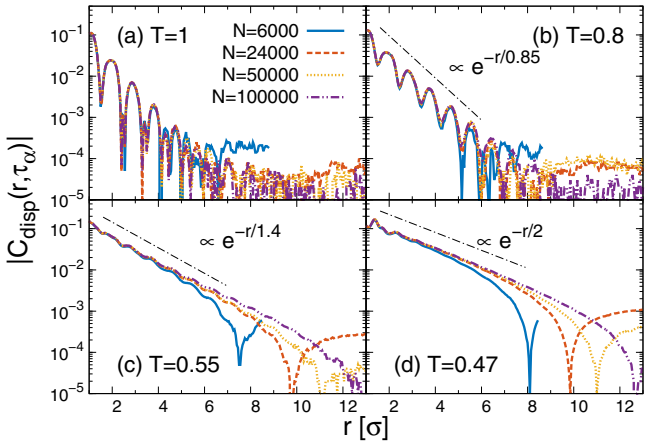

FIG. 3. Modulus of the spatial correlation function of the displacement field for different systems. In the lower two panels, (c) and (d), clear dip points emerge as the correlation function turns from positive to negative. The decay of the correlation and the dip points show a clear system size dependence.

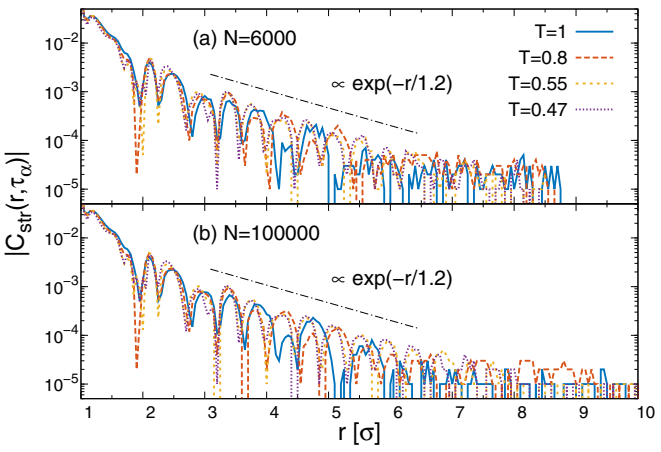

FIG. 4. Spatial correlation function of atomic-level shear-stress field for (a) $N = 6000$ particles system and (b) $N = 100\,000$ particles system. The decay of the correlation function does not show a clear system-size dependence.

IV. DISCUSSION AND CONCLUSION

The shear-stress correlation function can be connected with the viscosity by considering that

$$\eta = \frac{1}{Vk_BT}\int_0^\infty \left\langle \left[\sum_i \sigma_i^{xy}(t)\right]\left[\sum_i \sigma_i^{xy}(0)\right]\right\rangle dt$$
$$= \frac{1}{Vk_BT}\int_0^\infty dt \int_V dr \left\langle \sum_{ij} \sigma_i^{xy}(t)\sigma_j^{xy}(0)\delta(r-|\vec{r}_i-\vec{r}_j|)\right\rangle, \quad (3)$$

where $\sigma_i^{xy} = mv_i^x v_i^y + \sum_j r_{ij}^x F_{ij}^y$, is the atomic-level shear stress of atom i, with F_{ij} being the force exerted by atom j on atom i. The term inside the brackets $\langle\cdots\rangle$ actually is the cross term for different times in the spatial correlation function (see its definition in Sec. II). Thus, the time convergence of the stress autocorrelation function for viscosity measurement is determined by the correlation function $C_{\text{stress}}(r,t)$. To study the spatiotemporal fluctuation of $C_{\text{stress}}(r,t)$ which relates to the viscosity calculation, we plot $4\pi r^2 C_{\text{stress}}(r,t)$ in Fig. 5.

First, the oscillation behavior of the correlation is observable, with the periodicity coinciding with the atomic diameter. With time elapsing, this oscillation propagates to larger distances. As reported recently [55,56], the front propagation speed corresponds to that of a longitudinal sound wave. As the longitudinal sound velocity depends weakly on temperature, the shape of the shear-stress wave does not differ so much between a high temperature (left panels) and low temperature (right panels) at short time scales. In long time scales ($t \gg \tau_\alpha$), the longest propagation distance for a shear-stress wave is also quite close in normal liquids and highly supercooled liquids, although the viscosity of the system has drastically increased by more than three orders of magnitude for the temperature range illustrated.

To show the finite-size effect, we take two different system sizes, i.e., $N = 1600$ and $N = 100\,000$. For all time scales

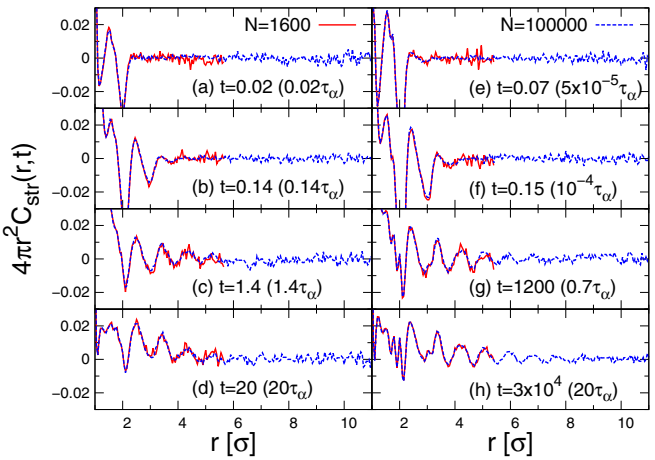

FIG. 5. Spatial correlation function of the atomic shear stress field at different times. The left panels (a)–(d) are for high-temperature liquid ($T = 1$), while the right panels (e)–(h) are for low-temperature liquid ($T = 0.47$). Two different system sizes are shown, i.e., $N = 1600$ and $N = 100\,000$, for a comparison.

and temperatures, no pronounced difference can be observed between the small and large systems. This indicates even in highly supercooled liquids the length scale required for the shear-stress relaxation is still small and cannot be detected by the small system size. For highly supercooled liquid ($T = 0.47$), in the long time limit, the longest distance where shear-stress waves can propagate to is about 8–10 σ, which coincides with the result of 10 interatomic distance found in normal liquids [55,57]. This length scale would be the maximum distance required for shear relaxation in these fragile liquids, and is almost temperature independent. As an estimation, we found the systems with box length larger than $9\,\sigma$ show almost the same saturated viscosity value (as vertical dashed line shown in Fig. 2).

This temperature-independent behavior of the length scale for the shear-stress reminds of the similar phenomenon for the structure, e.g., the unapparent change of the pair distribution function (or static structure factor) for liquids upon supercooling or even vitrification [5,24]. In the process of glass transition, although jamming of the systems in dynamics makes the atomic movement more collective, the configurational structure does not change significantly. As the attenuation of the shear-stress autocorrelation function is mainly determined by local static atomic structure, it exhibits both temperature and system-size insensitive behavior, as shown in Fig. 5.

We summarize the length scales extracted from finite-size dependent hydrodynamic value (from Figs. 1 and 2) and the spatial correlation functions (from Figs. 4 and 3) in Fig. 6. As in Fig. 6(a), the critical box length required for diffusion coefficient to reach the hydrodynamic value shows a diverging tendency upon supercooling, similar to the length scale of dynamic heterogeneity. The characteristic correlation length from displacement field also exhibits the same tendency [see Fig. 6(c)]. For viscosity, it is of an upper limit critical length scale, which eventually becomes smaller than the one of diffusivity at low temperature.

As the displacement field and the stress field defined here are isotopic, the characteristic length is a directional average of all the biased correlations, which actually is the common situation of atomic movement in viscous liquid, e.g., the form of stringlike movement (with the dimension of approximately 1.5 [58]). The length scales measured via displacement correlation function are much smaller than the length of correlated atoms measured by isotopic effect [30], but are comparable to the mean length of the mobile clusters [4] (up to around 2 atomic diameters). As the finite-size effect always detects the maximum length of any correlated movement, it gives the upper limit of the correlation length, whereas the spatial correlation functions give the lower limit.

A commonly used relation for self-diffusion coefficient and viscosity in molecular and atomic liquids is the Stokes-Einstein relation. The violation of this relation in supercooled liquids is usually connected with collective movement due to dynamic heterogeneity [17,29,59,60] or similarly the separation of fast and slow particles [29,30]. In the present system, the onset temperature for a significant break down of the SE relation is at around $T = 0.6$, as shown in Fig. 6(b). This temperature, actually, is also approximately the temperature where the characteristic length for the diffusivity exceeds the upper limit

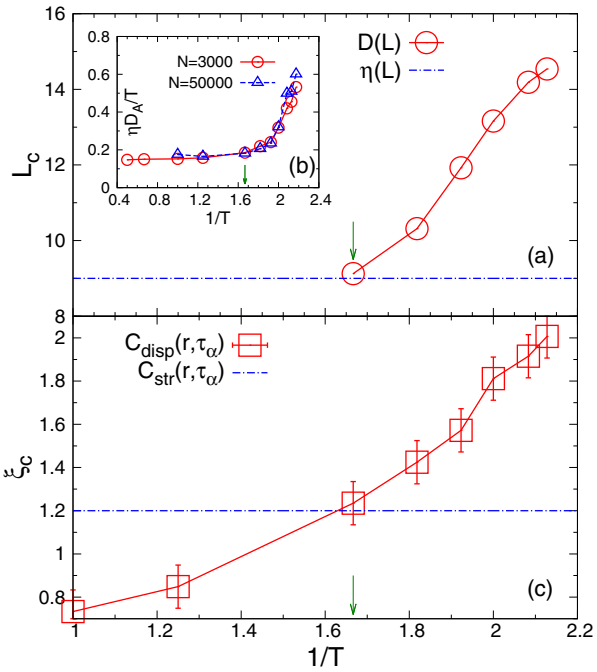

FIG. 6. (a) The critical box length required to reach the hydrodynamic value for the diffusivity (from Fig. 1) and the viscosity (from Fig. 2). The inset picture (b) is the Stokes-Einstein relation for a small and large box-length systems. (c) The correlation lengths calculated by exponential fitting of the spatial correlation function for displacement (Fig. 3) and atomic shear-stress (Fig. 4) fields. The green arrows mark the temperature point where the SER significantly brakes down.

length for the viscosity. In supercooled liquids, due to the sluggish dynamics, diffusion via collectively motion becomes more important and could eventually overwhelm the role played by configuration entropy. This competition is reflected in the different length scales required for diffusion and viscosity. Once the typical length scale from the displacement exceeds that from the stress field, diffusion process cannot be solely dominated by the configuration entropy any more. At this time, the SE relation begins to break down.

In conclusion, we utilize the finite-size method, combined with spatial correlation functions to investigate the underlying length scales for diffusion and viscous processes. For the diffusion a growing length scale is found with undercooling, consistent with the length scale of the dynamic heterogeneity; For shear viscosity the corresponding length scale saturates with undercooling and exhibits an almost temperature-independent behavior. The fluctuation of atomic-level shear stresses is found to be constrained to about 8–10 atomic diameters. This result is consistent with previous finite-size results for the structural relaxation time [44] and the static length gained by the structural frustration method [39,40]. We attribute the length scale of the shear relaxation process to the manifestation of the configurational entropy, while the one of the diffusion process to the collectivity due to dynamic heterogeneity. The competition between these two mechanisms can be seen in the decoupling of the length scales from the displacement and the shear-stress fields.

ACKNOWLEDGMENTS

The authors acknowledge financial support from the German Academic Exchange Service (DAAD) for funding through the DLR-DAAD programme under Grant No. 131. We thank H. R. Schober for many stimulating discussions throughout this work. The authors are also grateful to the computer resources provided by Konstanz Scientific Computer Cluster and Jülich Supercomputing Center.

[1] W. Götze, *Complex Dynamics of Glass-Forming Liquids A Mode-Coupling Theory* (Oxford University Press, Oxford, UK, 2009).
[2] W. Gotze and L. Sjogren, Rep. Prog. Phys. **55**, 241 (1992).
[3] W. Kob and H. C. Andersen, Phys. Rev. E **51**, 4626 (1995).
[4] C. Donati, J. F. Douglas, W. Kob, S. J. Plimpton, P. H. Poole, and S. C. Glotzer, Phys. Rev. Lett. **80**, 2338 (1998).
[5] L. Berthier and G. Biroli, Rev. Mod. Phys. **83**, 587 (2011).
[6] R. Yamamoto and A. Onuki, Phys. Rev. E **58**, 3515 (1998).
[7] M. D. Ediger, Annu. Rev. Phys. Chem. **51**, 99 (2000).
[8] C. Donati, S. C. Glotzer, and P. H. Poole, Phys. Rev. Lett. **82**, 5064 (1999).
[9] M. D. Ediger and P. Harrowell, J. Chem. Phys. **137**, 080901 (2012).
[10] N. Lacevic, F. W. Starr, T. B. Schroder, and S. C. Glotzer, J. Chem. Phys. **119**, 7372 (2003).
[11] A. S. Keys, A. R. Abate, S. C. Glotzer, and D. J. Durian, Nat. Phys. **3**, 260 (2007).
[12] E. Flenner and G. Szamel, Phys. Rev. Lett. **105**, 217801 (2010).
[13] E. Flenner, M. Zhang, and G. Szamel, Phys. Rev. E **83**, 051501 (2011).
[14] S. Karmakar, C. Dasgupta, and S. Sastry, Phys. Rev. Lett. **105**, 015701 (2010).
[15] X. J. Han and H. R. Schober, Phys. Rev. B **83**, 224201 (2011).
[16] F. Affouard, M. Descamps, L.-C. Valdes, J. Habasaki, P. Bordat, and K. L. Ngai, J. Chem. Phys. **131**, 104510 (2009).
[17] S. Sengupta, S. Karmakar, C. Dasgupta, and S. Sastry, J. Chem. Phys. **138**, 12A548 (2013).
[18] X. J. Han, J. G. Li, and H. R. Schober, J. Chem. Phys. **144**, 124505 (2016).
[19] L. Berthier, G. Biroli, D. Coslovich, W. Kob, and C. Toninelli, Phys. Rev. E **86**, 031502 (2012).
[20] W. Kob, S. Roldan-Vargas, and L. Berthier, Nat. Phys. **8**, 164 (2011).
[21] W.-S. Xu, Z.-Y. Sun, and L.-J. An, Phys. Rev. E **86**, 041506 (2012).
[22] E. Flenner and G. Szamel, Nat. Phys. **8**, 696 (2012).
[23] U. Balucani, R. Vallauri and T. Gaskell, Phys. Rev. A **35**, 4263 (1987).
[24] J. P. Hansen and I. R. Macdonald, *Theory of Simple Liquids*, 3rd ed. (Academic Press, Oxford, UK, 2005).

[25] A. Furukawa and H. Tanaka, Phys. Rev. Lett. **103**, 135703 (2009).
[26] A. Furukawa and H. Tanaka, Phys. Rev. E **86**, 030501(R) (2012).
[27] A. Furukawa, Phys. Rev. E **87**, 062321 (2013).
[28] L. Berthier, D. Chandler, and J. P. Garrahan, Europhys. Lett. **69**, 320 (2005).
[29] S. Sengupta, S. Karmakar, C. Dasgupta, and S. Sastry, J. Chem. Phys. **140**, 224505 (2014).
[30] H. R. Schober and H. L. Peng, Phys. Rev. E **93**, 052607 (2016).
[31] S. Sastry, P. G. Debenedetti, and F. H. Stillinger, Nature (London) **393**, 554 (1998).
[32] P. G. Debenedetti and F. H. Stillinger, Nature (London) **410**, 259 (2001).
[33] K. Kim and S. Saito, J. Chem. Phys. **138**, 12A506 (2013).
[34] S. Karmakar, C. Dasgupta, and S. Sastry, Annu. Rev. Condens. Matter Phys. **5**, 255 (2014).
[35] T. Kawasaki, T. Araki, and H. Tanaka, Phys. Rev. Lett. **99**, 215701 (2007).
[36] K. Watanabe and H. Tanaka, Phys. Rev. Lett. **100**, 158002 (2008).
[37] A. J. Dunleavy, K. Wiesner, and C. P. Royall, Phys. Rev. E **86**, 041505 (2012).
[38] P. Charbonneau and G. Tarjus, Phys. Rev. E **87**, 042305 (2013).
[39] F. Sausset and G. Tarjus, Phys. Rev. Lett. **104**, 065701 (2010).
[40] B. Charbonneau, P. Charbonneau, and G. Tarjus, Phys. Rev. Lett. **108**, 035701 (2012).
[41] V. Privman, *Finite Size Scaling and Numerical Simulation of Statistical Systems* (World Scientific, Singapore, 1990).
[42] K. Binder, Z. Phys. B **43**, 119 (1981).
[43] S. Karmakar, C. Dasgupta, and S. Sastry, Phys. Rev. Lett. **105**, 019801 (2010).
[44] S. Karmakar, C. Dasgupta, and S. Sastry, Proc. Natl. Acad. Sci. USA **106**, 3675 (2009).
[45] S. Plimpton, J. Comput. Phys. **117**, 1 (1995).
[46] J. P. Boon and S. Yip, *Molecular Hydrodynamics* (Courier Corporation, New York, 1980).
[47] B. Dünweg and K. Kremer, J. Chem. Phys. **99**, 6983 (1993).
[48] I.-C. Yeh and G. Hummer, J. Phys. Chem. B **108**, 15873 (2004).
[49] M. Kluge and H. R. Schober, Phys. Rev. B **70**, 224209 (2004).
[50] F. Puosi and D. Leporini, J. Chem. Phys. **136**, 164901 (2012).
[51] T. Narumi and M. Tokuyama, Philos. Mag. **88**, 4169 (2008).
[52] N. Lacevic, F. W. Starr, T. B. Schroder, V. N. Novikov, and S. C. Glotzer, Phys. Rev. E **66**, 030101(R) (2002).
[53] B. J. Alder and T. E. Wainwright, Phys. Rev. A **1**, 18 (1970).
[54] B. Doliwa and A. Heuer, Phys. Rev. E **61**, 6898 (2000).
[55] V. A. Levashov, J. R. Morris, and T. Egami, Phys. Rev. Lett. **106**, 115703 (2011).
[56] V. A. Levashov, J. R. Morris, and T. Egami, J. Chem. Phys. **138**, 044507 (2013).
[57] R. D. Mountain, J. Chem. Phys. **102**, 5408 (1995).
[58] C. Oligschleger and H. R. Schober, Phys. Rev. B **59**, 811 (1999).
[59] T. Kawasaki and A. Onuki, Phys. Rev. E **87**, 012312 (2013).
[60] S. C. Glotzer, V. N. Novikov, and T. B. Schroder, J. Chem. Phys. **112**, 509 (2000).